Martin Brodrecht[a], Edda Klotz[a], Christina Lederle, Hergen Breitzke, Bernd Stühn, Michael Vogel* and Gerd Buntkowsky*

A Combined Solid-State NMR, Dielectric Spectroscopy and Calorimetric Study of Water in Lowly Hydrated MCM-41 Samples

https://doi.org/10.1515/zpch-2017-1030
Received September 8, 2017; accepted November 9, 2017

Abstract: The processes of drying mesoporous silica materials and their refilling with water have been examined by magic-angle spinning (MAS) solid-state NMR, broadband dielectric spectroscopy (BDS), and differential scanning calorimetry (DSC). It is shown that different drying protocols strongly influence the amount and types of hydroxy-species inside the pores. It is found that a very good vacuum ($\approx 10^{-6}$ bar) is necessary to remove all H_2O molecules from the silica matrices in order to accurately refill them with very low amounts of water such as e.g. a mono- or submonolayer coverage of the surface. Time-dependent ^{1}H-NMR-spectra recorded after loading the samples indicate a very specific course of water first existing in a bulk-like form inside the pores and then distributing itself through the pores by hydrogen bonding to surface silanol groups. After assuring accurate sample loading, we were able to investigate lowly hydrated samples of water confined in MCM-41 via DCS and BDS at temperatures below the freezing point of free bulk-water (0 °C) and find two non-crystallizing water species with Arrhenius behavior and activation energies of 0.53 eV (51.1 kJ/mol).

Keywords: broadband dielectric spectroscopy; confinement; solid-state NMR; water; wetting.

[a]**Martin Brodrecht and Edda Klotz:** These authors contributed equally to this work.
***Corresponding authors: Michael Vogel,** Institut für Festkörperphysik, Technische Universität Darmstadt, 64289 Darmstadt, Germany, e-mail: michael.vogel@physik.tu-darmstadt.de; and **Gerd Buntkowsky,** Institut für Physikalische Chemie, Technische Universität Darmstadt, 64287 Darmstadt, Germany, e-mail: gerd.buntkowsky@chemie.tu-darmstadt.de
Martin Brodrecht and Hergen Breitzke: Institut für Physikalische Chemie, Technische Universität Darmstadt, 64287 Darmstadt, Germany
Edda Klotz, Christina Lederle and Bernd Stühn: Institut für Festkörperphysik, Technische Universität Darmstadt, 64289 Darmstadt, Germany

1 Introduction

Due to its variety of anomalies and properties that are not fully understood, even after tens of years of studies, water still provides an interesting field of research. The reason for the anomalous behavior of bulk water is widely believed to be found in the so-called no man's land between 150 and 135 K [1, 2]. To prevent water from crystallizing in that temperature regime, it is often studied inside a geometrically confined geometry.

There is a great variety of confinement types [3] which influence, e.g. freezing and melting properties of confined liquids [4–7]. In particular water or binary water mixtures in confinement have been thoroughly investigated by broadband dielectric spectroscopy (BDS) [8–15], NMR [16–23] and differential scanning calorimetry (DSC) [9, 24]. The interpretation of the results of those various studies is, however, still discussed controversially [3]. Our recent approach of investigating water confined in MCM-41 shows [25], that the discrepancies existing between some results on water in lowly hydrated confinement could very well be the consequence of different ways of sample preparation. In order to gain a deeper insight into this process, the drying of the MCM-41 material as well as the process of filling water into the pores have been investigated via ^{1}H-NMR and BDS. Those measurements reveal the immense importance of the protocol for sample drying and filling, especially when preparing lowly hydrated samples, where a coexistence of surface ("non-freezable") and bulk-water like ("freezable") water exists (for details see the reviews [18, 26] and references therein). The hydrated samples prepared by applying the obtained knowledge were then investigated with BDS to reveal the dynamics of water layers near the pore surface.

2 Experimental details

MCM-41 was synthesized based on a method of Grünberg et al. [27] and Grün et al. [28] with a precursor of tetradecyltrimethylammoniumbromid (MTAB) with a C-chain length of C14. 0.55 g (0.14 eq.) of MTAB was dissolved in 140 mL deionized water using ultrasonic. The mixture was heated to 35 °C (308 K) and 2.9 mL ammonia solution (25%) was added. The solution was stirred for another 10 min under treatment of ultrasonic. 3.00 g (1.00 eq.) tetraethoxysilane (TEOS) was slowly added. After the addition was complete the suspension was further treated with ultrasonic for 1 h. The resulting suspension was transferred into a Teflon-bottle and aged at 80 °C (353 K) for 72 h. After ageing the white precipitate was filtered off. The solid was washed with deionized water and diethyl ether and afterwards dried over night at 100 °C (373 K). The leftover template was removed at 650 °C (923 K) by calcination.

The porosity and specific surfaces area of the material was characterized by nitrogen adsorption at 77 K, employing a Thermo Fisher Scientific Surfer BET analyzer. From the BET measurements a specific pore volume of 0.77 cm^3/g (Gurvich), a specific surface area of 1000.2 m^2/g (BET) and a specific pore diameter of 3.6 nm (BJH) were determined.

CP-MAS solid state NMR measurements were carried out at room temperature on a Bruker AVANCE II+ spectrometer at 400 MHz proton resonance frequency, employing a Bruker 4 mm double resonance probe. Measurements were performed utilizing a Bruker background suppression pulse sequence employing a 30° pulse, a delay time of 10 s and a MAS spinning rate of 10 kHz [29].

DSC experiments were performed using a Q1000 from TA Instruments. The samples were placed in hermetically sealed aluminum pans and the data was acquired during heating runs at 10 K/min. The complex dielectric permittivity, $\varepsilon(\omega)=\varepsilon'(\omega)=i\varepsilon''(\omega)$, was measured using a Novocontrol Alpha-N High Resolution Dielectric Analyzer. The sample temperature was controlled by a Novocontrol Quatro Cryosystem with a temperature stability better than ±0.2 K and an absolute accuracy of ±0.5 K. A sample cell similar to that introduced by Wagner and Richert [30] was employed. The distance of the capacitor plates was 400 µm.

The dielectric permittivity was analyzed by fitting to a conductivity term and a sum of Cole–Cole (CC) functions

$$\varepsilon^*(\omega)=\varepsilon_\infty+\frac{\sigma_{dc}}{i\varepsilon_0\omega}+\sum_{j=1}^{N}\frac{\Delta\varepsilon_j}{1+(i\omega\tau_j)^{\alpha_j}}$$

here, ε_∞ is the high-frequency limit of the permittivity, ε_0 the vacuum permittivity, and σ_{dc} denotes the dc conductivity. The CC processes are characterized by their relaxation strength $\Delta\varepsilon_j$, relaxation time τ_j, and width parameter α_j. Several previous studies showed that CC functions well describe symmetrically broadened loss peaks associated with heterogeneous dynamics of confined water [8, 9, 12, 13]. Here, we use CC fits mainly to determine the peak positions and, thus, the relaxation times τ_j.

3 Sample preparation

3.1 Drying of MCM-41 materials

The synthesized and untreated MCM-41 material was filled into a tared 4 mm NMR rotor ($m_{rotor}=744.1$ mg). Subtracting the rotor mass from the total mass of the filled rotor ($m_{total}=780.5$ mg) results in the sample mass of $m_{sample}=36.4$ mg.

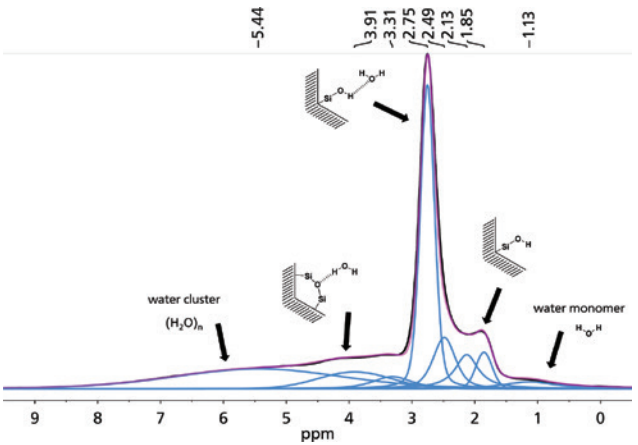

Fig. 1: ^{1}H solid-state NMR spectrum of water in a conventionally stored and not dried sample of MCM-41 at 10 kHz (black). Deconvolution (blue), sum of deconvolution (pink), and assignment of water species to the peaks according to Grünberg et al. [25].

To check the hydration state of the untreated sample ^{1}H-MAS-NMR measurements were carried out (Figure 1).

The chemical shifts of the water species in these spectra are determined by the local environments of the H-atoms. At high fields (0.8–1.5 ppm) single, isolated water molecules can be found. Surface bound silanol groups are located at around 1.7–1.8 ppm. The signals from 2.1 to 2.8 ppm are assigned to water molecules associated to the surface silanol groups, whereas clustered water is found at low fields (4.5–5.5 ppm). The chemical shift values of the observed peaks are the result of the weighted average of the individual shifts of the different hydroxy-species in the sample and are assigned accordingly [25].

In order to investigate the behavior of well-defined amounts of guest molecules, the host surface has to be prepared into a well-defined state. This means that the sample has to be dried until only silanol groups are present.

Since mesoporous silica materials are strongly hygroscopic and tend to absorb water fast, all drying procedures were performed with the sample inside the NMR rotor. Treating the sample outside of the rotor and transferring it for the measurement would expose the sample to humidity, which results in a wet sample again. The ^{1}H-NMR measurements after different drying protocols are compared in Figure 2.

First the sample was exposed to high temperatures (180 °C/453 K) over night. The resulting spectrum is practically identical with the spectrum of the untreated sample. It can therefore be concluded that high temperatures alone are not

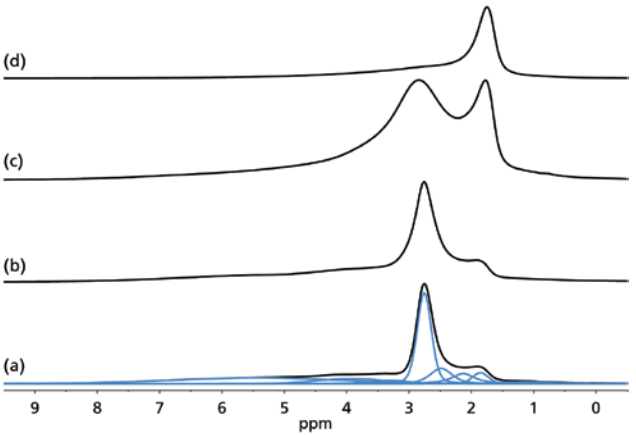

Fig. 2: ^{1}H solid-state NMR spectra of the MCM-41 samples at 10 kHz: (a) Untreated sample and corresponding deconvolution (blue). (b) Sample dried at 180 °C (453.15 K) under atmospheric pressure for 24 h. (c) Sample dried at room temperature under mild vacuum (10^{-1} mbar, 24 h). (d) Sample dried at room temperature under high vacuum (10^{-6} mbar, 24 h). All spectra are normalized to equal height.

sufficient to remove water from the MCM-41 sample sufficiently. Second, the same sample was treated with moderate vacuum (10^{-1} mbar) over night. The ^{1}H-NMR spectrum shows a significant decrease of surface associated water species and the loss of all water clusters. Consequently water was removed from the sample but surface associated water is still present. Subsequently the sample was treated using a turbomolecular pump (10^{-6} mbar) for 24 h. The resulting ^{1}H-NMR spectrum shows the absence of surface associated water. Only the isolated silanol groups remain, so all water was removed sufficiently. Finally, we wish to note that there is a weak broad signal between ca. 4 and 2 ppm, which indicates the presence of a small amount of very strongly bound water molecules, which we attribute to trapped water. Similar results of trapped water molecules, which could not be removed by heating to ca. 100 °C under vacuum were also reported previously by some of us [25].

Now the mass of the dried sample can be determined by subtracting the rotor mass ($m_{rotor} = 744.1$ mg) from the new total mass of the dried sample including the rotor ($m_{total(dry)} = 779.7$ mg). Therefore the dry sample mass was found to be $m_{sample(dry)} = 35.6$ mg.

In parallel to NMR, BDS is used to study the suitability of different drying methods for MCM-41 materials. Figure 3 shows the dielectric loss of MCM-41 samples that have been dried by different means and for different periods of time. A sample that has been dried in a vacuum oven at 10^{-3} bar exhibits a

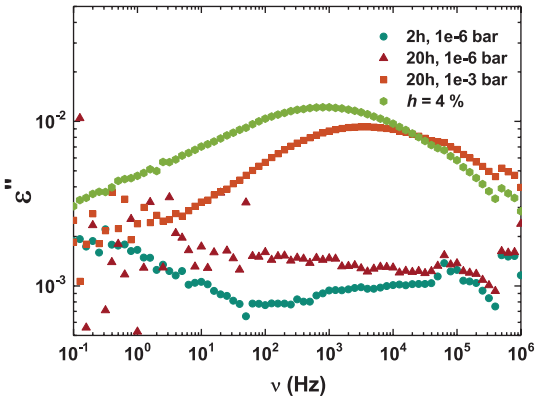

Fig. 3: Dielectric loss $\varepsilon''(\nu)$ of MCM-41 C14 samples at $T = 150$ K after different drying methods. Specifically, the samples have been dried using a turbomolecular pump at a vacuum level of 10^{-6} bar and room temperature for 2 h and 20 h, respectively, or using a vacuum oven at vacuum level of 10^{-3} bar and room temperature for 20 h. For comparison, the dielectric loss is shown for a sample that has been completely dried and deliberately filled to a hydration level of $h = 4\%$.

distinct dielectric signal, even after a long drying time. This signal arises from the rotational motion of remaining water molecules. Actually, the dielectric loss of this sample resembles that of a sample, which has been deliberately filled to a hydration level of $h = 4\%$. By contrast, samples that have been dried for 2 or 20 h with a turbomolecular pump at 10^{-6} mbar show no dielectric signal at all, indicating that essentially all water has been removed.

3.2 Sample loading

Based on the BET results 100% sample loading was defined as completely filling the determined pore volume of the sample. The pore volume was found to be 0.765 cm^3/g, therefore adding 0.765 µL of water for each mg of sample is defined as 100% pore filling, for the present sample under test. A well-defined amount of water was added onto the sample using a micro pipette. After loading the sample, the rotor was closed with a spin cap and the ^{1}H-NMR measurements were started. In order to monitor the diffusion process into equilibrium, one spectrum per hour was recorded, until no change was observed anymore.

After equilibrium was reached, the rotor was removed from the spectrometer and the sample inside the rotor was dried again, according to the procedure described above. The dried sample was loaded again with slightly higher amounts of water and the ^{1}H-spectra were recorded as described, until the equilibrium was

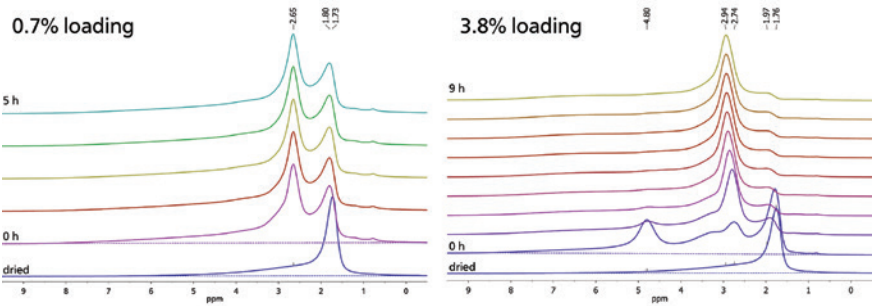

Fig. 4: ^{1}H solid-state NMR spectra of the MCM-41 at low filling states at 10 kHz. Sample filled with 0.7% (left) and 3.8% (right) of water referred to the pore volume. Spectra measured at time intervals of 1 h. Bottom: the dry sample. To show that there is spectral intensity at low fields the straight lines in the dried and 0 h spectra show the NMR baseline.

reached again. Nominal sample loadings of 0.7%, 3.8%, 7.5% and 15.0% have been used. During these repeated drying and loading cycles no signs of irreversible pore changes were observed.

First ^{1}H-spectra for two low filling states of 0.7% and 3.8% are depicted in Figure 4. At nominally 0.7% filling a peak of the silanol groups (1.75 ppm), and a peak of surface associated water at 2.65 ppm can be found. Consequently only a part of the surface seems to be covered with water. The spectra do not show any change after the first hours. Therefore the sample reaches an equilibrium state rather quickly.

The filling with nominally 3.8% of water shows bulk water at 4.8 ppm immediately after filling, which vanishes within the first hour. In addition it also shows the peak at around 2.74 ppm and the silanol peak at 1.76 ppm. After several hours the latter peak vanishes and the peak at 2.74 ppm shifts to lower fields. This indicates that the water is inhomogeneously distributed within the sample immediately after loading, forming bulk water outside the pores or close to the pore opening. Over time the water molecules diffuse inside the silica until finally the inner surface (note: the outer surface of the silica particles is ca. three orders of magnitude smaller than the inner surface and can be neglected) is completely covered by a monomolecular water layer, indicated by the growing peak at around 2.7 ppm and the decreasing silanol peak. Equilibrium is reached after 4 h. Filling the sample with nominally 7.5%, results in a spectrum similar to the previous case of 3.8% filling. However, the bulk water peak at around 4.7 ppm is still present after equilibrium is reached (Figure 5). Furthermore, the silanol peak is decreased but still present. That is, despite the presence of bulk water, the sample surface still possesses regions which are either not yet reached on this time scale or are completely inaccessible to water molecules.

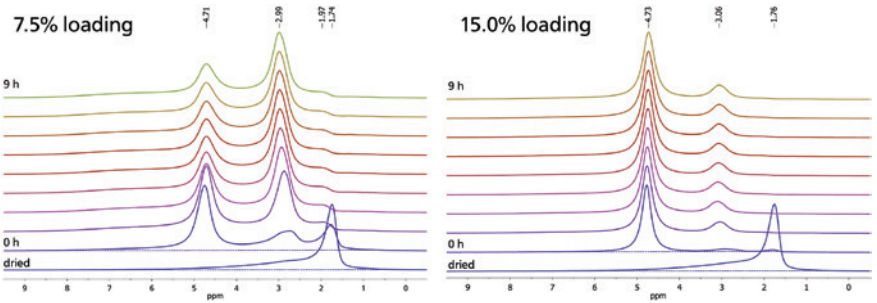

Fig. 5: ^{1}H solid-state NMR spectra of the MCM-41 at low filling states at 10 kHz. Sample filled with 7.5% (left) and 15.0% (right) of water referred to the pore volume. Spectra measured at time intervals of 1 h. Bottom: the dry sample.

It is known that many pore systems tend to fill several pores completely whereas some pores are only covered with monolayers of water [25]. But it can be concluded that a filling of 7.5% results in an equilibrium state in which bulk-like water is present.

To complete these experiments we investigated also 15.0% filling (Figure 5). Here the equilibrium is reached quickly. The silanol groups disappear completely during pore filling. Even the surface associated species are dominated by the bulk water peak at 4.73 ppm.

Therefore a nominal filling of 15.0% seems to be way too high to investigate the surface associated water species. On the other hand a nominal filling of at least 15.0% should be used to investigate the bulk-like water species inside the pores, i.e. those water molecules, which are not in direct contact with the silica surface, but surrounded by other water molecules. For investigating only the surface associated water species a loading between 3.8 and 7.5% is ideal.

3.3 Water dynamics in weakly hydrated MCM-41

First, we use DSC to study water behaviors in mesoporous silica. Figure 6 shows heating curves obtained for a dry and two weakly hydrated MCM-41 C14 samples. While the dry sample and the one with a low hydration level of $h = 5\%$ yield no calorimetric signal, the sample with a moderate filling of $h = 35\%$ shows a small endothermic peak at $T_m = 221$ K, indicating melting of a small ice fraction. Thus, at low fillings, no freezable water with bulk-like properties exists since essentially all molecules are adsorbed on the inner silica surfaces, consistent with the above MAS NMR results. Only at higher hydration levels, adsorbed water coexists with

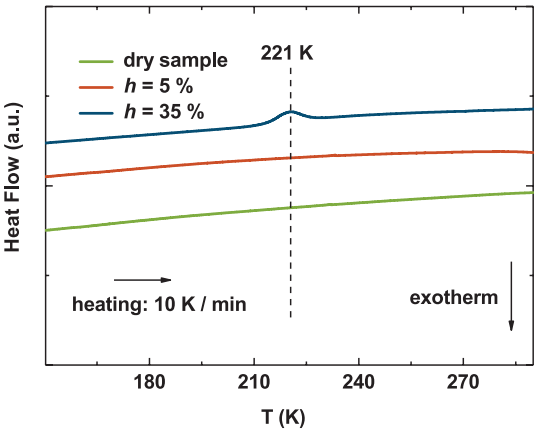

Fig. 6: DSC heating curves for MCM-41 C14 at different filling states. Results for various hydration levels h are vertically shifted for clarity. The heating rate was 10 K/min. While no calorimetric signals are observed for low hydration levels, a small melting peaking at $T_m = 221$ K is observed for $h = 35\%$, as marked by the dashed line.

freezable water, which resides at sufficiently large distances to the pore wall and freezes upon cooling. The melting temperature $T_m = 221$ K observed for the latter partially filled sample is in agreement with results of previous studies on completely filled MCM-41 C14, which reported melting points between 220 and 230 K, in harmony with the Gibbs–Thomson equation for phase transition in confined geometries [24, 31].

Next, BDS is used to investigate the rotational dynamics of water in weakly hydrated MCM-41 C14. Figure 7 shows the dielectric loss $\varepsilon''(\nu)$ for samples with $h = 4\%$ and $h = 38\%$. The sample with the lower hydration level exhibits, apart from a conductivity contribution, a single process in the studied temperature range. This process will hereafter be denoted as P1. It shows CC form and shifts to lower frequencies when decreasing the temperature. Its width parameter α decreases from 0.5 to 0.3 upon cooling, indicative of a broad distribution of correlation times. For the sample with the higher water content, it is evident that the dielectric loss cannot be described by a single process. Rather, a slower second process appears, while the first one loses intensity. This second process will be referred to as P2 in the following. Both processes of this sample can be approximately described by CC peaks with width parameters α comparable to that found for $h = 4\%$. In Figure 8, we display the relaxation times τ of the observed processes. For $h = 4\%$, we see that P1 follows an Arrhenius law with an activation energy of $E_a = 0.53$ eV (51 kJ/mol). Since the typical bond energy of an OH···O–hydrogen bond is ca. 20 kJ/mol and for a molecular water rotation

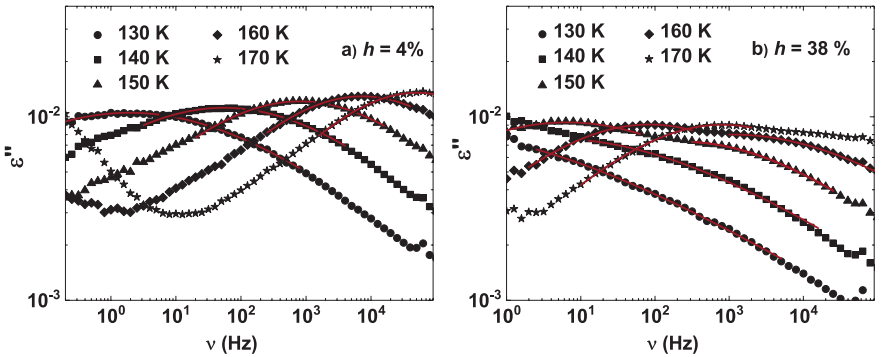

Fig. 7: Dielectric loss $\varepsilon''(\nu)$ characterizing water reorientation in MCM-41 at different temperatures: (a) $h = 4\%$ and (b) $h = 38\%$. The lines are interpolations using one (4%) and two (38%) CC processes, respectively.

at least two hydrogen bonds need to be broken, we tentatively assign this activation energy to the hydrogen bonds of the water molecule. However, the exact mechanism of water reorientation in water remains elusive. For $h = 38\%$, P1 shows comparable behavior with somewhat larger τ values. P2 exhibits substantially longer relaxation times, which can also be described by an Arrhenius law. The obtained activation energy of $E_a = 0.53$ eV for P2 agrees within the error margins with that of P1. The present results for P1 and P2 well agree with previous findings in a BDS study on water in silica pores with a larger diameter of ~3.6 nm [13], see Figure 8. There, it was shown in more detail that P2 increases in expense of process P1 when increasing the hydration level until the latter process eventually vanishes at water contents higher than that of the present study. Moreover, the origin of deviations from an Arrhenius law at sufficiently high hydration levels h was discussed [13]. However, this issue remains very controversial [3, 9–15], e.g. it was attributed to a transition between high-density and low-density forms of liquid water or to a crossover from primary (α) to secondary (β) relaxation.

Thus, present and previous findings yield a consistent picture of water dynamics in mesoporous silica. P1 is the only process at low hydration levels, while it disappears for high water contents. Hence, we attribute this process to the reorientation of water molecules, which are adsorbed on the inner silica surface and form at least one hydrogen bond to the silanol-groups. At intermediate hydration levels, such water molecules coexist with water molecules that do belong to a well-established network. Then, P1 coexists with P2, which can be assigned to the latter species. P2 is the only process at high hydration levels, at which all water molecules are part of a three-dimensional hydrogen-bond network. In

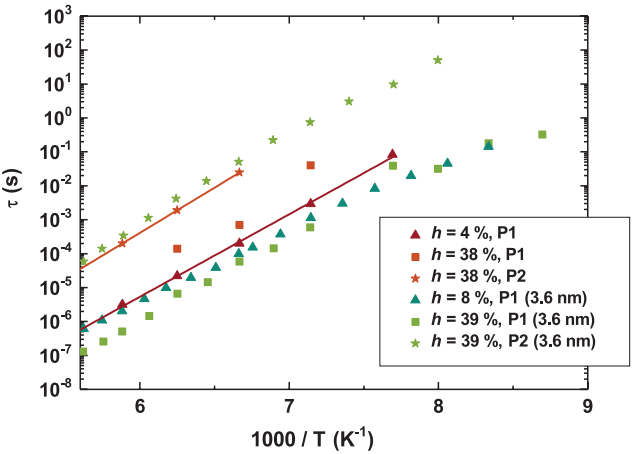

Fig. 8: Relaxation times τ for the observed dynamic processes of water in MCM-41 C14 at the indicated hydration levels h. For comparison, results from a previous BDS study on water in larger MCM-41 pores ($d = 3.6$ nm) are included [13]. The lines are Arrhenius fits, yielding activation energies of $E_a = 0.48$ eV (46.3 kJ/mol) for process P1 at $h = 4\%$ and $E_a = 0.52$ eV (50.2 kJ/mol) for process P2 at $h = 38\%$.

narrow confinements, this network is, however, affected by the inner surfaces and, hence, deviates from that of bulk water. Consequently, P2 corresponds to the widely known relaxation process of water in different types of confinements [23, 32, 33].

4 Conclusion

In conclusion, it has been shown that sample preparation and thus the sample history has a major influence on the water structure and distribution in lowly hydrated MCM-41 samples. The investigation of those lowly hydrated samples with DSC and BDS shows that even at temperatures far below the freezing point in confinement, no crystallization takes place. Instead, for hydration levels below 30% we find a single amorphous water species that can be assigned to H_2O molecules hydrogen bound to the silanol groups of the pore walls. With increasing amounts of water, a second, dynamically distinguishable species arises that represents water in hydrogen-bond networks near interfaces. Altogether, the combination of CP-MAS solid state NMR, DSC and BDS leads to a better understanding of the pore filling, and thereby of the different water species existing inside MCM-41 confinement and their dynamics.

Acknowledgements: Financial support by the Deutsche Forschungsgemeinschaft in the framework of Forschergruppe FOR 1583 through grants Bu-911/18-1/2, STU 191/6-2 and Vo-905/8-1/2 is gratefully acknowledged.

References

1. P. H. Poole, F. Sciortino, U. Essmann, H. E. Stanley, Nature **360** (1992) 324.
2. O. Mishima, H. E. Stanley, Nature **396** (1998) 329.
3. S. Cerveny, F. Mallamace, J. Swenson, M. Vogel, L. Xu, Chem. Rev. **116** (2016) 7608.
4. E. Gedat, A. Schreiber, J. Albrecht, T. Emmler, I. Shenderovich, G. H. Findenegg, H. H. Limbach, G. Buntkowsky, J. Phys. Chem. B **106** (2002) 1977.
5. W. Masierak, T. Emmler, E. Gedat, A. Schreiber, G. H. Findenegg, G. Buntkowsky, J. Phys. Chem. B **108** (2004) 18890.
6. C. Alba-Simionesco, B. Coasne, G. Dosseh, G. Dudziak, K. Gubbins, R. Radhakrishnan, M. Sliwinska-Bartkowiak, J. Phys. Condens. Mat. **18** (2006) 15.
7. M. Febles, N. Perez-Hernandez, C. Perez, M. L. Rodriguez, C. Foces-Foces, M. V. Roux, E. Q. Morales, G. Buntkowsky, H. H. Limbach, J. D. Martin, J. Am. Chem. Soc. **128** (2006) 10008.
8. R. Bergman, J. Swenson, Nature **403** (2000) 283.
9. H. Jansson, J. Swenson, Eur. Phys. J. E **12** (2003) 51.
10. A. Faraone, L. Liu, C.-Y. Mou, C.-W. Yen, S.-H. Chen, J. Chem. Phys. **121** (2004) 10843.
11. A. Spanoudaki, B. Albela, L. Bonneviot, M. Peyrard, Eur. Phys. J. E **17** (2005) 21.
12. J. Hedström, J. Swenson, R. Bergman, H. Jansson, S. Kittaka, Eur. Phys. J. Spec. Top. **141** (2007) 53.
13. J. Sjöström, J. Swenson, R. Bergman, S. Kittaka, J. Chem. Phys. **128** (2008) 154503.
14. F. Mallamace, C. Corsaro, P. Baglioni, E. Fratini, S.-H. Chen, J. Phys.: Condens. Matter **24** (2012) 064103.
15. J. Swenson, S. Cerveny, J. Phys.: Condens. Matter **27** (2014) 033102.
16. A. Vyalikh, T. Emmler, E. Gedat, I. Shenderovich, G. H. Findenegg, H. H. Limbach, G. Buntkowsky, Solid State Nucl. Mag. **28** (2005) 117.
17. F. Mallamace, M. Broccio, C. Corsaro, A. Faraone, U. Wanderlingh, L. Liu, C.-Y. Mou, S. H. Chen, J. Chem. Phys. **124** (2006) 161102.
18. G. Buntkowsky, H. Breitzke, A. Adamczyk, F. Roelofs, T. Emmler, E. Gedat, B. Grünberg, Y. Xu, H.-H. Limbach, I. Shenderovich, Phys. Chem. Chem. Phys. **9** (2007) 4843.
19. A. Vyalikh, T. Emmler, B. Grünberg, Y. Xu, I. Shenderovich, G. H. Findenegg, H. H. Limbach, G. Buntkowsky, Z. Phys. Chem. **221** (2007) 155.
20. A. Vyalikh, T. Emmler, I. Shenderovich, Y. Zeng, G. H. Findenegg, G. Buntkowsky, Phys. Chem. Chem. Phys. **9** (2007) 2249.
21. M. Sattig, M. Vogel, J. Phys. Chem. Lett. **5** (2014) 174.
22. M. F. Harrach, B. Drossel, W. Winschel, T. Gutmann, G. Buntkowsky, J. Phys. Chem. C **119** (2015) 28961.
23. M. Rosenstihl, K. Kämpf, F. Klameth, M. Sattig, M. Vogel, J. Non-Cryst. Solids **407** (2015) 449.
24. S. Jähnert, F. V. Chávez, G. Schaumann, A. Schreiber, M. Schönhoff, G. Findenegg, Phys. Chem. Chem. Phys. **10** (2008) 6039.

25. B. Grünberg, T. Emmler, E. Gedat, I. Shenderovich, G. H. Findenegg, H.-H. Limbach, G. Buntkowsky, Chem. Eur. J. **10** (2004) 5689.
26. R. Richert, Annu. Rev. Phys. Chem. **62** (2011) 65.
27. B. Grünberg, A. Grünberg, H.-H. Limbach, G. Buntkowsky, App. Magn. Res. **44** (2013) 189.
28. M. Grün, K. K. Unger, A. Matsumoto, K. Tsutsumi, Microporous Mesoporous Mater. **27** (1999) 207.
29. D. G. Cory, W. M. Ritchey, J. Magn. Res. **80** (1988) 128.
30. H. Wagner, R. Richert, J. Phys. Chem. B **103** (1999) 4071.
31. S. Kittaka, S. Ishimaru, M. Kuranishi, T. Matsuda, T. Yamaguchi, Phys. Chem. Chem. Phys. **8** (2006) 3223.
32. S. Cerveny, G. A. Schwartz, R. Bergman, J. Swenson, Phys. Rev. Lett. **93** (2004) 245702.
33. J. Swenson, H. Jansson, R. Bergman, Phys. Rev. Lett. **96** (2006) 247802.